

Lithium Halide Adducts of Imidotellurium(IV) Ligands: Synthesis and X-ray Structures of $[\text{Li}(\text{THF})_2\text{L}](\mu_3\text{-I})[\text{Li}(\text{L})]$ [$\text{L} = \text{}^t\text{BuNTe}(\mu\text{-N}^t\text{Bu})_2\text{TeN}^t\text{Bu}$] and $[(\text{THF})_3\text{Li}_3(\mu_3\text{-I})\{\text{Te}(\text{N}^t\text{Bu})_3\}]$

Tristram Chivers,* Masood Parvez, and Gabriele Schatte

Department of Chemistry, University of Calgary, 2500 University Drive N.W.,
Calgary, Alberta, Canada T2N 1N4

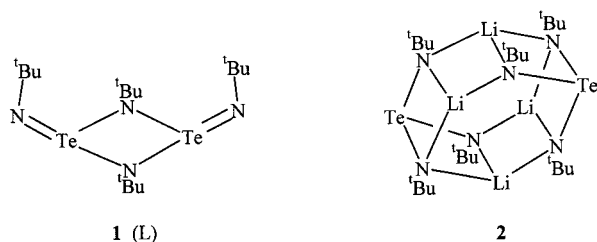
Received July 14, 2000

The reaction of the chelating ligand ${}^t\text{BuNTe}(\mu\text{-N}^t\text{Bu})_2\text{TeN}^t\text{Bu}$ (**L**) with LiI in THF yields $[\text{Li}(\text{THF})_2\text{L}](\mu_3\text{-I})[\text{Li}(\text{L})]$ (**3**). This complex is also formed by the attempted oxidation of $[\text{Li}_2\text{Te}(\text{N}^t\text{Bu})_3]_2$ with I_2 . An X-ray analysis of **3** reveals that the tellurium diimide dimer acts as a chelating ligand toward (a) $[\text{Li}(\text{THF})_2]^+$ cations and (b) a molecule of LiI . An extended structure is formed via weak $\text{Te}\cdots\text{I}$ interactions [3.8296(7)–3.9632(7) Å] involving both μ_3 -iodide counterions and the iodine atoms of the coordinated LiI molecules. Crystal data: **3**, triclinic, space group $P\bar{1}$, $a = 10.1233(9)$ Å, $b = 15.7234(14)$ Å, $c = 18.8962(17)$ Å, $\alpha = 86.1567(16)^\circ$, $\beta = 84.3266(16)^\circ$, $\gamma = 82.9461(16)^\circ$, $V = 2965.8(5)$ Å³, $Z = 2$. The oxidation by air of $[\text{Li}_2\text{Te}(\text{N}^t\text{Bu})_3]_2$ in toluene produces the radical $\{\text{Li}_3[\text{Te}(\text{N}^t\text{Bu})_3]_2\}^{\bullet}$, which exhibits an ESR spectrum consisting of a septet of decuplets ($g = 2.00506$, $a(^{14}\text{N}) = 5.26$ G, $a(^7\text{Li}) = 0.69$ G). The complexes $[(\text{THF})_3\text{Li}_3(\mu_3\text{-X})\{\text{Te}(\text{N}^t\text{Bu})_3\}]$ (**4a**, X = Cl; **4b**, X = Br; **4c**, X = I) are obtained from the reaction of $[\text{Li}_2\text{Te}(\text{N}^t\text{Bu})_3]_2$ with lithium halides in THF. The iodide complex, **4c**, has a highly distorted, cubic structure comprised of the pyramidal $[\text{Te}(\text{N}^t\text{Bu})_3]^{2-}$ dianion which is linked through three $[\text{Li}(\text{THF})]^+$ cations to I^- . Crystal data: **4c**, triclinic, space group $P\bar{1}$, $a = 12.611(8)$ Å, $b = 16.295(6)$ Å, $c = 10.180(3)$ Å, $\alpha = 98.35(3)^\circ$, $\beta = 107.37(4)^\circ$, $\gamma = 108.26(4)^\circ$, $V = 1829(2)$ Å³, $Z = 2$.

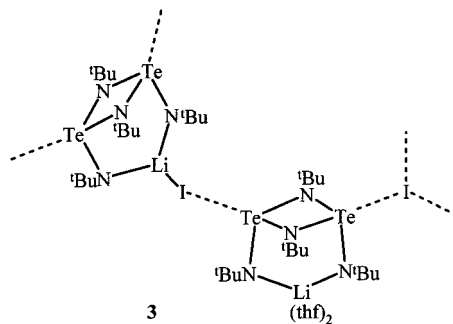
Introduction

The tellurium diimide dimer **1** is a useful reagent for the preparation of new, thermally stable tellurium–nitrogen compounds.¹ Recent investigations have shown that **1** can function either as a chelating ligand, or as a bridging ligand, toward Ag^+ or Cu^+ .² Furthermore, Cu^+ ions promote *cis* → *trans* isomerization of **1**. The redistribution reaction of **1** with TeCl_4 produces the imidotellurium(IV) dichloride, $[\text{Cl}_2\text{Te}(\mu\text{-N}^t\text{Bu})_2\text{TeCl}_2]_3$.³ In addition, the reactions of **1** with the nucleophilic reagents KO^tBu or LiNH^tBu generate the novel anions $[\text{Te}(\text{N}^t\text{Bu})_2(\text{O}^t\text{Bu})]^-$ or $[\text{Te}(\text{N}^t\text{Bu})_3]^{2-}$, respectively.^{4,5} As its dilithium derivative, the latter adopts the dimeric cyclic ladder structure, **2**.⁵ Similar structures have been established for the sulfur⁶ and selenium⁷ analogues of **2**. These sulfur- or selenium-containing clusters are readily oxidized by oxygen or iodine, to give deep blue (E = S) or green (E = Se) radicals $\{\text{Li}_3[\text{E}(\text{N}^t\text{Bu})_3]_2\}^{\bullet}$ that exhibit characteristic (septet of decuplets) ESR spectra.^{8,9} In the case

of the sulfur species, further oxidation generates the sulfur(VI) compound, $\text{S}(\text{N}^t\text{Bu})_3$, which is isoelectronic with SO_3 .^{8,10}



The objective of this investigation was to compare the behavior of **2** upon oxidation with that of the sulfur and selenium analogues. The initial results of the reaction with I_2 revealed the formation of $[\text{Li}(\text{THF})_2\text{L}](\mu_3\text{-I})[\text{Li}(\text{L})]$ (**3**, L = **1**), a novel



coordination complex of **1**, with an extended structure that incorporated two different types of $\text{Li}\cdots\text{I}$ interactions. Subse-

* To whom correspondence may be sent. Fax: (403) 289-9488. E-mail: chivers@ucalgary.ca.

- (1) Chivers, T.; Gao, X.; Parvez, M. *J. Am. Chem. Soc.* **1995**, *117*, 2359.
- (2) (a) Chivers, T.; Parvez, M.; Schatte, G. *Angew. Chem., Int. Ed.* **1999**, *38*, 2217. (b) Chivers, T.; Parvez, M.; Schatte, G. *Inorg. Chem.* **1999**, *38*, 5171.
- (3) Chivers, T.; Enright, G. D.; Sandblom, N.; Schatte, G.; Parvez, M. *Inorg. Chem.* **1999**, *38*, 5431.
- (4) Chivers, T.; Gao, X.; Parvez, M. *Inorg. Chem.* **1996**, *35*, 553.
- (5) (a) Chivers, T.; Gao, X.; Parvez, M. *Angew. Chem., Int. Ed. Engl.* **1995**, *34*, 2549. (b) Chivers, T.; Gao, X.; Parvez, M. *Inorg. Chem.* **1996**, *35*, 4336.
- (6) Fleischer, R.; Freitag, S.; Pauer, F.; Stalke, D. *Angew. Chem., Int. Ed. Engl.* **1996**, *35*, 204.
- (7) Chivers, T.; Parvez, M.; Schatte, G. *Inorg. Chem.* **1996**, *35*, 4094.
- (8) Fleischer, R.; Freitag, S.; Stalke, D. *J. Chem. Soc., Dalton Trans.* **1998**, 193.
- (9) Brask, J. K.; Chivers, T.; McGarvey, B.; Schatte, G.; Sung, R.; Boeré, R. T. *Inorg. Chem.* **1998**, *37*, 4633.

- (10) Fleischer, R.; Rothenberger, A.; Stalke, D. *Angew. Chem., Int. Ed. Engl.* **1997**, *36*, 1107.

quently, **3** was obtained in high yield from the treatment of **1** with LiI in THF. We also describe the synthesis and multinuclear NMR characterization of lithium halide adducts of **2**, and the X-ray structure of $[(\text{THF})_3\text{Li}_3(\mu_3\text{-I})\{\text{Te}(\text{N}^i\text{Bu})_3\}]$ (**4c**).

Experimental Section

The reagents $\text{BuNTe}(\mu\text{-N}^i\text{Bu})_2\text{TeN}^i\text{Bu}^3$ and $[\text{Li}_2\text{Te}(\text{N}^i\text{Bu})_3]_2^5$ were prepared by following the literature procedures. Lithium halides, LiX (X = Cl, Br, and I), were obtained from Aldrich and dried under vacuum before use. Solvents were dried with appropriate drying agents and distilled onto molecular sieves before use. All reactions were carried out under an argon atmosphere using standard Schlenk techniques or a drybox.

^1H NMR spectra were recorded on Bruker ACT 200 and DRX 400 spectrometers, and chemical shifts are reported relative to Me_4Si in CDCl_3 , ^{125}Te , ^7Li , and ^{13}C NMR spectra were measured at 25 °C in C_7D_8 , C_6D_6 , or $\text{C}_4\text{D}_8\text{O}$ on Bruker DRX 400 and AMX 300 spectrometers, by using a 5 mm broadband probe (BBI) and the appropriate operating frequencies for the observed nuclei. The samples were locked on 6.98 ppm (C_7D_8) and 3.58 ppm ($\text{C}_4\text{D}_8\text{O}$), externally referenced to K_2TeO_3 in D_2O , and referred to Me_2Te and 1.0 M LiCl in D_2O and $\text{C}_4\text{D}_8\text{O}$, respectively. For the ^{125}Te and ^{13}C NMR spectra, delays of 1.5 and 3 s, respectively, were applied. Line-broadening parameters, used in the exponential multiplication of the free induction decays, were 5 to 0.5 Hz. Chemical shifts with a positive sign are correlated with shifts to high frequencies (downfield) of the reference compound. ESR spectra were recorded on a Bruker ESP 300e spectrometer equipped with a NMR magnetometer and a microwave counter. Spectral simulations were carried out using the WINEPR Sim Fonia program provided by Bruker. Elemental analyses were performed by Analytical Services, Chemistry Department, University of Calgary.

Synthesis of $[\text{Li}(\text{THF})_2\text{L}][\mu_3\text{-I}][\text{Li}(\text{L})]$ [3**, L = $\text{Te}_2(\text{N}^i\text{Bu})_4$]. (a) **Reaction of $\text{BuNTe}(\mu\text{-N}^i\text{Bu})_2\text{TeN}^i\text{Bu}$ (**1**) and LiI.** A colorless solution of LiI (0.074 g, 0.556 mmol) in THF (10 mL) was added dropwise to the stirring red solution of **1** (0.300 g, 0.556 mmol) in *n*-hexane (10 mL) at 23 °C. A red-orange precipitate formed initially. Upon further addition of the LiI/THF solution, most of this precipitate dissolved, and the color of the solution changed to a darker red. The reaction mixture was stirred for 2 h. The volatile materials were removed under vacuum, and the solid was washed twice with cold *n*-hexane (−10 °C) to give the red-orange product **3**·THF (0.352 g, 0.225 mmol, 81%). ^1H NMR (C_6D_6): δ 3.56 (m, THF, 12 H), 1.59 (s, ^iBu , 36 H), 1.40 (m, THF, 12 H), 1.26 (s, ^iBu , 36 H). ^1H NMR (d_8 -THF): δ 1.47 (s, ^iBu , 36 H), 1.45 (s, ^iBu , 36 H). ^{13}C NMR (d_8 -THF): δ 62.81 [$\text{C}(\text{CH}_3)_3$], 58.68 [$\text{C}(\text{CH}_3)_3$], 37.23 [$\text{C}(\text{CH}_3)_3$], 36.15 [$\text{C}(\text{CH}_3)_3$]. ^7Li NMR (d_8 -THF): δ −1.01. ^{125}Te NMR (d_8 -THF): δ 1689. CHN analyses indicated the loss of ca. two molecules of THF from solid samples. Anal. Calcd for $\text{C}_{36}\text{H}_{80}\text{N}_8\text{Li}_2\text{I}_2\text{Te}_4\text{O}$: C, 30.47; H, 5.68; N, 7.89. Found: C, 30.57; H, 6.14; N, 7.93.**

Crystals of **3**, suitable for X-ray crystallography, were obtained from a solution of **3**·THF in *n*-hexane/THF (6 mL, 1:4 by volume) stored at −27 °C for 14 days.

(b) **Reaction of $\text{Li}_2[\text{Te}(\text{N}^i\text{Bu})_3]$ (**2**) and I_2 .** A solution of I_2 (0.286 g, 1.13 mmol) in THF (5 mL) was added to a solution of **2** (0.400 g, 1.13 mmol) in *n*-hexane (15 mL) at −78 °C. After 0.5 h the reaction mixture was allowed to reach 23 °C to give an orange precipitate. After an additional 2.5 h, the solid (0.403 g) was separated by decantation and was dried under vacuum. Crystals suitable for X-ray analysis were obtained from a d_8 -THF solution (ca. 1 mL) of this product (0.060 g) that was stored in an NMR tube for 3 weeks. The crystals were identified as **3**·0.45 H_2O . ^1H NMR (in d_8 -THF, 25 °C): δ 1.473 (^iBu), 1.414 (^iBu) (intensity ratio 1:1). ^{13}C NMR (in d_8 -THF, 25 °C): δ 61.50 [$\text{C}(\text{CH}_3)_3$], 59.07 [$\text{C}(\text{CH}_3)_3$], 37.70 [$\text{C}(\text{CH}_3)_3$], 35.84 [$\text{C}(\text{CH}_3)_3$]. ^7Li NMR (in d_8 -THF, 25 °C): δ 0.68.

Synthesis of $[(\text{THF})_3\text{Li}_3(\mu_3\text{-I})\{\text{Te}(\text{N}^i\text{Bu})_3\}]$ (4c**).** A solution of LiI (0.075 g, 0.564 mmol) in THF (10 mL) was added dropwise to a solution of $[\text{Li}_2\text{Te}(\text{N}^i\text{Bu})_3]_2$ (0.200 g, 0.282 mmol) in *n*-hexane (10 mL) at 23 °C. The yellow solution was stirred for 1.5 h. The volume of the solution was reduced to 10 mL under vacuum. Storage of the resulting solution at −29 °C yielded **4c** (0.383 g, 0.54 mmol, 96%) as pale yellow, X-ray quality crystals. NMR data for **4c** are summarized in

Table 1. NMR Data for **4a–c**

δ (^1H)	δ (^{13}C)	δ (^7Li)	δ (^{125}Te)
4a^a			
1.41 (thf)	25.85 [$\text{O}(\text{CH}_2\text{CH}_2)_2$]	2.38	1515.1
1.56 (^iBu)	37.97 [$\text{C}(\text{CH}_3)_3$]		
	<i>c</i> [$\text{C}(\text{CH}_3)_3$]		
3.74 (thf)	68.88 [$\text{O}(\text{CH}_2\text{CH}_2)_2$]		
4b^b			
1.42 (thf)	25.78 [$\text{O}(\text{CH}_2\text{CH}_2)_2$]	2.31	1523.7
1.55 (^iBu)	37.87 [$\text{C}(\text{CH}_3)_3$]		
	55.23 [$\text{C}(\text{CH}_3)_3$]		
3.87 (thf)	69.29 [$\text{O}(\text{CH}_2\text{CH}_2)_2$]		
4c^a			
1.40 (thf)	25.80 [$\text{O}(\text{CH}_2\text{CH}_2)_2$]	2.06	1538.2
1.51 (^iBu)	37.79 [$\text{C}(\text{CH}_3)_3$]		
	55.36 [$\text{C}(\text{CH}_3)_3$]		
3.87 (thf)	69.46 [$\text{O}(\text{CH}_2\text{CH}_2)_2$]		
0.88 ($\text{CH}_3\text{CH}_2\text{CH}_2$) ₂	14.67 ($\text{CH}_3\text{CH}_2\text{CH}_2$) ₂		
1.26 ($\text{CH}_3\text{CH}_2\text{CH}_2$) ₂	23.38 ($\text{CH}_3\text{CH}_2\text{CH}_2$) ₂		
and ($\text{CH}_3\text{CH}_2\text{CH}_2$) ₂	32.30 ($\text{CH}_3\text{CH}_2\text{CH}_2$) ₂		
	$[\text{Li}_2\text{Te}(\text{N}^i\text{Bu})_3]_2^b$		
1.34 (^iBu)	37.85 [$\text{C}(\text{CH}_3)_3$]	0.77	1522.6 ^d
1.29 (^iBu) ^d	56.09 [$\text{C}(\text{CH}_3)_3$]	2.67, 1.55	
		(2:1) ^d	

^a In C_6D_6 at 25 °C. ^b In C_7D_8 at 25 °C. ^c Not observed. ^d In $\text{C}_4\text{D}_8\text{O}$ at 25 °C; the previously reported value (δ ^{125}Te = 152.6 in C_7D_8 at 25 °C)^{5a} is incorrect.

Table 1. The ^1H and ^{13}C NMR spectra, as well as CHN analysis, indicated the presence of 0.5 *n*-hexane in the product. Anal. Calcd for $\text{C}_{27}\text{H}_{58}\text{N}_3\text{Li}_3\text{IO}_3\text{Te}$: C, 43.35; H, 7.81; N, 5.62. Found: C, 42.33; H, 7.88; N, 6.14.

Synthesis of $[(\text{THF})_3\text{Li}_3(\mu_3\text{-X})\{\text{Te}(\text{N}^i\text{Bu})_3\}]$ (4a**, X = Cl; **4b**, X = Br).** The complexes **4a** and **4b** were obtained in 45% and 99% yields, respectively, from the reaction of **2** with the appropriate lithium halide using the conditions described above for **4c**. The initial product of the LiCl reaction contained unreacted **2** even after a reaction time of 18 h. Pure **4a** was obtained by recrystallization of this product from THF at −27 °C. NMR data for **4a** and **4b** are summarized in Table 1. The CHN analysis for **4b** indicated the loss of ca. one molecule of THF. Anal. Calcd for $\text{C}_{20}\text{H}_{43}\text{N}_3\text{Li}_3\text{BrO}_2\text{Te}$: C, 40.10; H, 7.40; N, 7.17. Found: C, 39.71; H, 7.43; N, 7.45. The CHN analyses for **4a** indicated the loss of two THF molecules.¹¹ Anal. Calcd for $\text{C}_{16}\text{H}_{35}\text{Li}_3\text{ClO}_2\text{Te}$: C, 40.59; H, 7.52; N, 8.95. Found: C, 41.62; H, 7.65; N, 7.68.

X-ray Structure Determinations. The measurements for **3**·THF were determined on a Bruker AXS SMART 1000 CCD diffractometer, while those for **4c** were carried out on a Rigaku AFC6S diffractometer.

Complex 3. A red-orange prism-like crystal of **3**, having the approximate dimensions of 0.40 × 0.20 × 0.14 mm, was coated with oil (Paratone 8277, Exxon) and was mounted on a glass fiber. Data were measured using ϕ (0.4° per frame, 20 s exposures for a full 360° rotation at X = 30° and for an 80° rotation at X = −30°) and ω (0.4° per frame, 20 s exposures, X = 80°, four series [ϕ = 0°, 90°, 180°, 270°] of 75 frames) scans.

The first 40 ϕ -scan frames were re-collected at the end of the data collection to monitor for decay; a decay of less than 0.1% was observed, and thus no decay correction was employed. Cell parameters were retrieved using SMART software,¹² refined with SAINT,¹³ using 5969 observed reflections from the data collection. Data reduction was performed with the Bruker-AXS SHELXTL XPREP software,¹⁴ which corrects for Lorentz and polarization effects. The linear absorption

(11) Crystals of **4a** lose THF even more easily than those of **4b**. Consequently, it was difficult to obtain an accurate CHN analysis for **4a**.

(12) SMART V 5.0, Software for the CCD Detector System; Bruker AXS, Inc.: Madison, WI, 1998.

(13) SAINT V 5.0, Software for the CCD Detector System (Area-Detector Integration Software); Bruker AXS, Inc.: Madison, WI, 1998.

(14) SHELXTL-NT 5.1, XPREP, Program Library for Structure Solution and Molecular Graphics; Bruker AXS, Inc.: Madison, WI, 1998.

Table 2. Crystallographic Data for **3** and **4c**

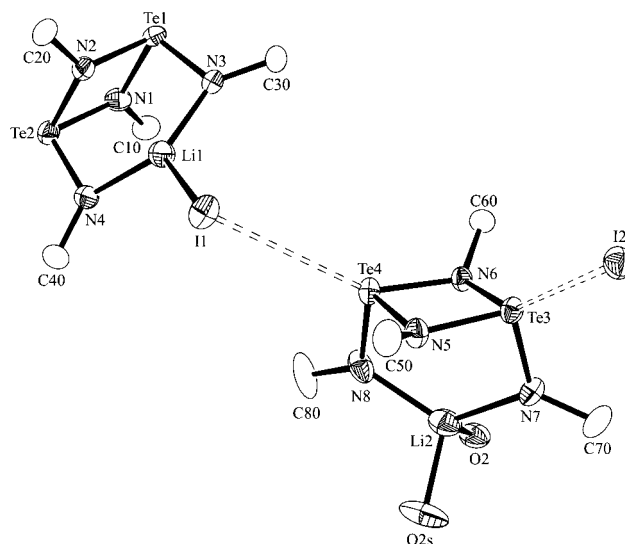
	3	4c
formula	C ₄₀ H ₈₈ N ₈ Li ₂ I ₂ Te ₄ O ₂	C ₂₇ H ₅₈ N ₃ TeLiI ₃ O ₃
fw	1491.26	748.10
cryst syst	triclinic	triclinic
<i>T</i> , °C	−80	−103
space group	<i>P</i> 1	<i>P</i> 1 (No. 2)
<i>a</i> , Å	10.1233(9)	12.611(8)
<i>b</i> , Å	15.7234(14)	16.295(6)
<i>c</i> , Å	18.8962(17)	10.180(3)
α, deg	86.1567(16)	98.35(3)
β, deg	84.3266(16)	107.37(4)
γ, deg	82.9461(16)	108.26(4)
<i>V</i> , Å ³	2965.8(5)	1829(2)
<i>Z</i>	2	2
ρ _{calc} , g cm ^{−3}	1.670	1.358
μ(Mo Kα), cm ^{−1}	30.24	16.84
λ, Å	0.71073	0.71069
<i>R</i> ₁ [<i>I</i> > 2σ(<i>I</i>)]	0.0278	0.038 ^a
w <i>R</i> ₂	0.0720	0.126 ^b

$$^a R_1 = \sum |F_o| - |F_c| / \sum |F_o|. \quad ^b wR_2 = \{[\sum w(F_o^2 - F_c^2)^2] / [\sum w(F_o^2)]\}^{1/2}.$$

coefficient, μ , for Mo K α is 3.024 mm^{−1}. An empirical (face-indexed) absorption correction, based on the transmission factor range 0.3776–0.6769, was applied (SADABS).¹⁵ The intensities of 14 258 reflections were collected. The data were merged (all equivalents and Friedel opposites, $R_{\text{int}} = 0.0263$) to provide 10 053 unique data ($R_{\sigma} = 0.0319$) and 8325 observed ($I > 2\sigma(I)$) reflections. The ranges of indices were $-11 \leq h \leq 11$, $-18 \leq k \leq 19$, and $0 \leq l \leq 22$, which correspond to a θ -range of 1.08–24.71°.

The structure was solved using direct methods (SIR-97)¹⁶ and refined by the full-matrix least-squares method on F^2 with SHELXL97-2.¹⁷ One of THF solvent molecules was disordered over two sites with partial occupancy factors of 0.642(8) and 0.358(8), respectively. The non-hydrogen atoms were refined anisotropically. Hydrogen atoms were included at geometrically idealized positions and were not refined. Neutral-atom scattering factors for non-hydrogen atoms and anomalous dispersion coefficients are contained in the SHELXTL-NT 5.1 program library.¹⁵ X-ray crystallographic data for **3** are presented in Table 2.

Complex 4c. A pale yellow crystal of **4c** (0.60 × 0.40 × 0.32 mm), coated with a Paratone oil, was mounted on a glass fiber. The cell constants and an orientation matrix for data collection were determined from the setting angles of 25 carefully centered reflections in the range 38.45° < 2θ < 41.80°. Scans of (1.52 + 0.34 tan θ) were made at a scan speed of 8.0° min^{−1} to a maximum 2θ value of 55.1°. Of the 8834 reflections collected, 8444 were unique ($R_{\text{int}} = 0.050$) and 5721 [$I > 2\sigma(I)$] were observed. The data were corrected for Lorentz and polarization effects, and an empirical absorption correction was applied. The structure was solved by direct methods¹⁸ and expanded using Fourier techniques.¹⁹ The non-hydrogen atoms were refined anisotropically. Hydrogen atoms were included at geometrically idealized positions and were not refined. Conventional atomic scattering factors, corrected for anomalous dispersion, were used²⁰ and allowance was made for anomalous dispersion. All calculations for data reduction were

**Figure 1.** ORTEP diagram of the asymmetric unit of **3** with the atomic numbering scheme. For clarity only the α -carbon atoms of tBu groups are shown.

performed using teXsan,²¹ and refinement was completed by full-matrix least-squares calculations with the aid of SHELXL97-2.¹⁷ X-ray crystallographic data for **4c** are presented in Table 2.

Results and Discussion

Synthesis, Spectroscopic Characterization, and Crystal Structure of [Li(THF)₂L](μ -I)[Li(L)] (3**, L = **1**).** The reaction of the tellurium diimide dimer **1** with an equimolar amount of LiI in THF produced **3**, as an orange solid in >80% yield. The ¹H and ¹³C NMR spectra of **3** in *d*₈-THF showed two types of NtBu environments, with approximately equal intensities, in addition to the presence of coordinated THF ligands. The ⁷Li NMR spectrum of **3** in *d*₈-THF exhibited a singlet at δ 0.49.

The X-ray structure determination of orange crystals, grown from a THF solution, revealed the composition of **3** to be {Li(THF)₂[Te₂(NtBu)₄](μ -I)[LiI[Te₂(NtBu)₄]]}. An ORTEP drawing of the asymmetric unit is depicted in Figure 1. Pertinent bond lengths and bond angles are summarized in Table 3. The tellurium diimide dimer **1** behaves as a chelating ligand toward the lithium centers which exist in two forms, viz. neutral LiI molecules and [Li(THF)₂]⁺ cations. This is the first example of a complex in which **1** chelates a single metal center. Both the iodide counterions and the iodine atoms of neutral LiI molecules engage in weak Te...I interactions to give an extended structure (see Figure 2).

The mean terminal Te–N bond lengths in the two different forms of the ligand, **1**, in complex **3** are identical (1.900 Å), whereas the mean values for the bridging Te–N bond distances are significantly different, 2.040 Å in [1•Li(THF)₂]⁺ and 2.027 Å in [1•LiI], respectively (cf. 1.876(10) and 2.081(8) Å in **1**).¹ Chelation to LiI or Li(THF)₂⁺ does, however, convert the *endo*-*endo* arrangement of terminal NtBu groups to the *exo*,*exo* configuration (Figure 1). The same configuration is observed in the silver(I) complex [Ag₂L₂](CF₃SO₃)₂ (L = **1**), in which the ligand is chelated to a Ag₂²⁺ unit.^{2a} Although the bond angles in the four-membered Te₂N₂ rings in **3** are similar to the corresponding values for **1** [\angle NTeN] = 76.3° vs 75.6 (4)°, [\angle TeNTe] = 103.5 vs 101.0 (6)°, chelation brings about a substantial contraction in the bond angle \angle N_{endo}TeN_{exo}. When **1** is coordinated to Li(THF)₂⁺, the mean value of this bond angle is 95.0° (range 94.61(17)–95.41(15)°, cf. 113.1(5)° in **1**),

(15) SADABS, V. 2.01: Software for Area-Detector Absorption and Other Corrections; Bruker AXS, Inc.: Madison, WI, 2000.

(16) Altomare, A.; Cascarano, M.; Giacovazzo, C.; Guagliardi, A.; Moliterni, G. G.; Burla, M. C.; Polidori, G.; Camalli, M.; Spagna, R. SIR97: A package for crystal structure solution by direct methods and refinement, Italy 1997.

(17) Sheldrick, G. M. SHELXL97-2: Program for the Solution of Crystal Structures, University of Göttingen, Göttingen, Germany, 1997.

(18) SIR92: Altomare, A.; Cascarano, M.; Giacovazzo, C.; Guagliardi, A. J. Appl. Crystallogr. 1993, 26, 343.

(19) DIRDIF94: Beurskens, P. T.; Admiraal, G.; Beurskens, G.; Bosman, W. P.; de Gelder, R.; Israel, R.; Smits, J. M. M. The DIRDIF-94 Program System. Technical Report of the Crystallography Laboratory; University of Nijmegen, The Netherlands, 1994.

(20) Cromer, D. T.; Waber, J. T. International Tables for Crystallography; Kynoch Press: Birmingham, England, 1974; Vol. IV, Table 2.2A, pp 71–98.

(21) teXsan, Single-Crystal Structure Analysis Software, Version 1.2; Molecular Structure Corp.: The Woodlands, TX, 1992.

Table 3. Selected Bond Lengths (Å) and Bond Angles (Deg) for **3**^a

Te(1)–N(1)	2.023(3)	Li(2)–O(1)	1.974(9)
Te(1)–N(2)	2.040(3)	Li(2)–O(2S)	2.034(11)
Te(1)–N(3)	1.901(3)	Li(1)–N(3)	2.074(9)
Te(2)–N(1)	2.006(4)	Li(1)–N(4)	2.117(8)
Te(2)–N(2)	2.041(3)	Li(2)–N(7)	2.211(9)
Te(2)–N(4)	1.901(4)	Li(2)–N(8)	2.171(10)
Te(3)–N(5)	2.041(3)	I(1)–Li(1)	2.695(8)
Te(3)–N(7)	1.900(3)		
Te(3)–N(6)	2.048(3)	I(2)···Te(1)	3.9251(7)
Te(4)–N(5)	2.032(3)	Te(2)···I(2)*	3.8679(7)
Te(4)–N(6)	2.038(3)	I(1)···Te(4)	3.9632(7)
Te(4)–N(8)	1.900(3)	Te(3)···I(2)''	3.8296(7)
N(3)–Te(1)–N(1)	101.01(14)	N(7)–Te(3)–N(6)	94.69(14)
N(3)–Te(1)–N(2)	91.29(14)	N(7)–Te(3)–N(5)	95.41(15)
N(1)–Te(1)–N(2)	75.68(14)	N(6)–Te(3)–N(5)	76.60(13)
N(4)–Te(2)–N(1)	101.08(15)	N(8)–Te(4)–N(5)	94.61(17)
N(4)–Te(2)–N(2)	92.30(14)	N(8)–Te(4)–N(6)	95.11(14)
N(1)–Te(2)–N(2)	76.02(13)	N(5)–Te(4)–N(6)	77.01(13)
Te(2)–N(1)–Te(1)	105.08(15)	Te(4)–N(5)–Te(3)	103.06(15)
C(10)–N(1)–Te(2)	125.4(3)	C(50)–N(5)–Te(4)	122.8(3)
C(10)–N(1)–Te(1)	126.8(3)	C(50)–N(5)–Te(3)	123.3(3)
Te(1)–N(2)–Te(2)	103.22(14)	Te(3)–N(6)–Te(4)	102.58(14)
C(20)–N(2)–Te(1)	125.7(3)	C(60)–N(6)–Te(3)	119.9(2)
C(20)–N(2)–Te(2)	124.0(3)	C(60)–N(6)–Te(4)	120.9(2)
N(3)–Li(1)–N(4)	127.3(4)	C(70)–N(7)–Te(3)	120.1(3)
N(3)–Li(1)–I(1)	117.6(3)	Te(3)–N(7)–Li(2)	106.8(3)
N(4)–Li(1)–I(1)	114.7(3)	C(70)–N(7)–Li(2)	133.0(4)
C(30)–N(3)–Te(1)	121.3(3)	Te(4)–N(8)–Li(2)	107.6(2)
Te(1)–N(3)–Li(1)	104.0(3)	C(80)–N(8)–Te(4)	119.2(4)
C(30)–N(3)–Li(1)	133.9(3)	C(80)–N(8)–Li(2)	133.2(4)
Te(2)–N(4)–Li(1)	102.8(3)	N(8)–Li(2)–N(7)	124.5(4)
C(40)–N(4)–Li(1)	134.5(4)	O(1)–Li(2)–O(2S)	98.5(5)
C(40)–N(4)–Te(2)	121.1(3)	O(1)–Li(2)–N(7)	103.9(4)
		O(1)–Li(2)–N(8)	105.6(4)
		O(2S)–Li(2)–N(7)	109.7(6)
		O(2S)–Li(2)–N(8)	111.1(5)
N(1)–Te(1)···I(2)	132.30(17)	N(5)–Te(4)···I(1)	110.78(15)
N(2)–Te(1)···I(2)	106.49(16)	N(6)–Te(4)···I(1)	146.95(15)
N(3)–Te(1)···I(2)	125.92(17)	N(8)–Te(4)···I(1)	115.56(19)
N(1)–Te(2)···I(2)*	126.70(17)	Te(2)···I(2)*···Te(1)*	101.53(16)
N(2)–Te(2)···I(2)*	114.87(15)	Te(1)···I(2)*···Te(3)''	107.81(16)
N(4)–Te(2)···I(2)*	128.53(16)	Te(1)···I(2)*···Te(2)*	101.53(16)
N(5)–Te(3)···I(2)''	111.41(15)	Te(3)''···I(2)*···Te(2)*	119.68(16)
N(6)–Te(3)···I(2)''	147.66(15)	Li(1)–I(1)···Te(4)	93.03(16)
N(7)–Te(3)···I(2)''	114.96(17)		

^a Symmetry transformations used to generate equivalent atoms: *, $-x + 2, -y + 1, -z + 1$; '', $-x + 1, -y + 2, -z + 1$.

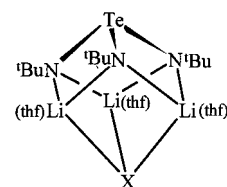
whereas two distinct values, 91.8 and 101.0°, are observed for $\angle N_{\text{endo}}\text{Te}N_{\text{exo}}$ when **1** is coordinated to LiI, i.e., a three-coordinate Li⁺ ion. The Te₂N₂ rings in the complex **3** are significantly less puckered than in the free ligand **1** (torsion angles: N(2)–Te(2)–N(1)–Te(1) = $-0.42(15)^\circ$, N(6)–Te(4)–N(5)–Te(3) = $-6.63(14)^\circ$, cf. $19.8(5)^\circ$ in **1**).¹ The tendency toward planarity of the Te₂N₂ ring was also observed for Cu⁺ and Ag⁺ complexes of **1**² and for the dimeric unit Cl₂Te(μ -N^t-Bu)₂TeCl₂.³

The Li⁺ ions of the Li(THF)₂⁺ fragment form an essentially symmetrical bridge [$d(\text{Li}–\text{N}) = 2.171(10)$ and $2.211(9)$ Å] between the two exocyclic N^tBu groups, with $\angle \text{NLiN} = 124.5(4)^\circ$. The three-coordinate Li⁺ ion of the coordinated LiI molecule also forms an almost symmetrical bridge involving significantly shorter Li–N bonds [$d(\text{Li}–\text{N}) = 2.074(9)$ and $2.117(8)$ Å, $\angle \text{NLiN} = 127.3(4)^\circ$].

The Li–I distance in the coordinated LiI molecule is 2.695(8) Å, which is significantly shorter than the distances observed for other LiI complexes.²⁰ The iodine atoms of the LiI molecules engage in weak interactions (μ_2 bridges) with a tellurium atom of the ligands **1** that are chelated to Li(THF)₂⁺ [$d(\text{Te}\cdots\text{I}) = 3.9632(7)$ Å]. The I[−] counterions of the latter fragment act as

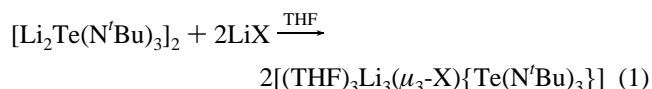
μ_3 bridges, linking the other tellurium atom of the fragment **1**·Li(THF)₂⁺ with one tellurium atom each of two **1**·LiI fragments [$d(\text{Te}\cdots\text{I}) = 3.8296(7)–3.9251(7)$ Å, cf. sum of van der Waals radii of Te and I = 4.04 Å].²³ These Te[⋯]I interactions are comparable to those found in β -Ph₂TeI₂ [$3.850(11)–3.926(11)$ Å],^{24a} α -Me₂TeI₂ [$3.659(3)–4.013(3)$ Å],^{24b} and (4-MeO-C₆H₄)₂TeI₂ [$3.6922(6)–3.9017(7)$ Å].^{24c} The extended structure that results from the Te[⋯]I interactions in **3** embraces two structural motifs, viz. a six-membered Te₄I₂ arrangement (ignoring the bridging N^tBu groups) located around the edges of the unit cell and a twelve-membered Te₆Li₂I₄ assembly with its center at 0, $1/2$, 0, which results in an infinite polymeric chain parallel to the *bc* plane when viewed down the *a*-axis (Figure 2).

Synthesis and Spectroscopic Characterization of [(THF)₃Li₃(μ_3 -X){Te(N^tBu)₃}] (4a, X = Cl; 4b, X = Br; 4c, X = I). The trisimidotellurite dianion in **2** is a useful reagent for incorporating main group elements, e.g., boron,^{5a} indium,²⁵ antimony,²⁶ or bismuth,²⁶ into Te–N rings via metathetical reactions with the appropriate halides. Lithium halides are the products of these reactions, and it is well established that these salts may become incorporated in Li–N clusters.^{5b,22,27} Consequently, in conjunction with our investigations of the reactions of **2** with halogens (vide infra), we also wished to determine whether this reagent would entrap lithium halides.



4a, X = Cl
4b, X = Br
4c, X = I

The lithium halide complexes **4a–c** were obtained in 45–96% yields by the *direct reaction* of the appropriate lithium halide with [Li₂Te(N^tBu)₃]₂ in THF/*n*-hexane (eq 1).²⁸ Stalke



et al. have previously reported the preparation of the corre-

- (22) Lithium–iodine distances in the range 2.760–2.979 Å have been reported for a variety of LiI complexes (see also ref 8): (a) Chivers, T.; Downard, A.; Parvez, M. *Inorg. Chem.* **1999**, *38*, 4347. (b) Raston, C. L.; Whitaker, C. R.; White, A. H. *J. Chem. Soc., Dalton Trans.* **1988**, 991. (c) Janssen, M. D.; Rijnberg, E.; de Wolf, C. A.; Hogerheide, M. P.; Kruis, D.; Kooijman, H.; Spek, A. L.; Grove, D. M.; van Koten, G. *Inorg. Chem.* **1996**, *35*, 6735. (d) van der Schaaf, P.; Hogerheide, M.; Spek, A.; Grove, D.; van Koten, G. *Chem. Commun.* **1992**, 1703.
- (23) Bondi, A. *J. Phys. Chem.* **1964**, *68*, 441.
- (24) (a) Alcock, N. W.; Harrison, W. D. *J. Chem. Soc., Dalton Trans.* **1984**, 869. (b) Chan, L. Y. Y.; Einstein, F. W. B. *J. Chem. Soc., Dalton Trans.* **1971**, 316. (c) Farran, J.; Alvarez-Larena, A.; Capparelli, M. V.; Piniella, J. F.; Germain, G.; Torres-Castellanos, L. *Acta Crystallogr., Sect. C: Cryst. Struct. Commun.* **1998**, *C54*, 995.
- (25) Chivers, T.; Schatte, G., unpublished results.
- (26) Chivers, T.; Parvez, M.; Schatte, G.; Yap, G. P. A. *Inorg. Chem.* **1999**, *38*, 1380.
- (27) (a) Fryzuk, M. D.; Giesbrecht, G. R.; Johnson, S. A.; Kickham, J. E.; Love, J. B. *Polyhedron* **1998**, *17*, 947. (b) Lambert, C.; Hampel, F.; Schleyer, P. v. R.; Davidson, M. G.; Snaith, R. *J. Organomet. Chem.* **1995**, *487*, 139. (c) Batsanov, A. S.; Davidson, M. G.; Howard, J. A. K.; Lamb, S.; Lustig, C.; Price, R. D. *Chem. Commun.* **1997**, 1211.

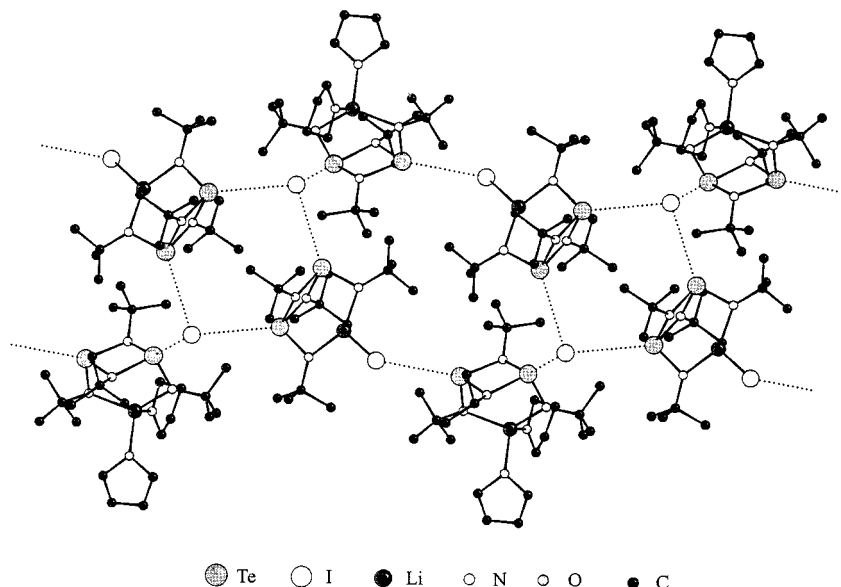


Figure 2. A view of the extended structure of **3** showing the two different types of Te...I interactions.

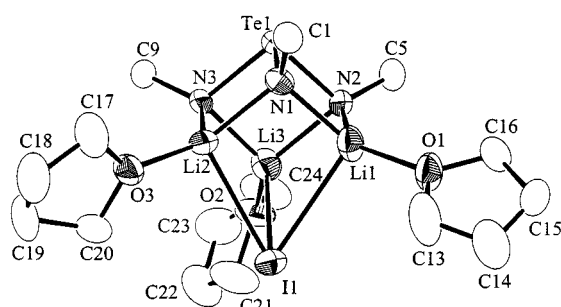


Figure 3. ORTEP diagram of **4c** with ellipsoids drawn at the 50% probability level. For clarity only the α -carbon atoms of 'Bu groups are shown.

sponding sulfur(IV) complexes, $[(\text{THF})_3\text{Li}_3(\mu_3\text{-X})\{\text{S}(\text{N}^t\text{Bu})_3\}]$ ($\text{X} = \text{Br}, \text{I}$), by the reaction of $[\text{Li}_2\text{S}(\text{N}^t\text{Bu})_3]_2$ with Br_2 or I_2 .^{8,29}

Compounds **4a–c** are moisture-sensitive, pale yellow solids that are soluble in *n*-hexane, toluene, or THF. Both the ^1H and ^{13}C NMR spectra indicate a single environment for the *tert*-butyl groups in **4a–c** (Table 1), as well as the presence of coordinated THF ligands. The ^1H NMR chemical shifts of the 'Bu groups occur at δ 1.51–1.56 (cf. δ 1.34 for $[\text{Li}_2\text{Te}(\text{N}^t\text{Bu})_3]_2$ in C_6D_6). The ^7Li NMR spectra for **4a–c** exhibit a singlet in the region δ 2.0–2.4, which is shifted downfield by 1.2–1.6 ppm compared to the resonance observed for $[\text{Li}_2\text{Te}(\text{N}^t\text{Bu})_3]_2$. The ^{125}Te NMR resonances for **4a–c** occur in the range δ 1515–1540. The congruence of the NMR data for all three derivatives implies that their structures are similar in solution. The observation of singlets in the ^1H , ^{13}C , and ^7Li NMR spectra suggests C_3 symmetry for these clusters.

Crystal Structure of $[(\text{THF})_3\text{Li}_3(\mu_3\text{-I})\{\text{Te}(\text{N}^t\text{Bu})_3\}]$ (4c**).** An ORTEP drawing of **4c** with the atomic numbering scheme is illustrated in Figure 3. Pertinent bond lengths and bond angles are summarized in Table 4. The structure consists of a highly distorted cube in which the pyramidal $[\text{Te}(\text{N}^t\text{Bu})_3]^{2-}$ dianion is linked to an iodide ion by three Li^+ cations, each of which is

Table 4. Selected Bond Lengths (Å) and Bond Angles (Deg) for **4c**

I(1)–Li(2)	2.901(10)	N(1)–Te(1)–N(3)	91.55(17)
I(1)–Li(3)	2.956(10)	N(1)–Te(1)–N(2)	92.85(18)
I(1)–Li(1)	2.958(10)	N(3)–Te(1)–N(2)	91.67(18)
Te(1)–N(1)	1.973(4)	Te(1)–N(1)–Li(2)	91.1(3)
Te(1)–N(3)	1.977(4)	Te(1)–N(1)–Li(1)	89.6(3)
Te(1)–N(2)	1.988(4)	Li(2)–N(1)–Li(1)	93.7(4)
O(1)–Li(1)	1.958(10)	Te(1)–N(2)–Li(1)	89.7(3)
O(2)–Li(3)	1.951(10)	Te(1)–N(2)–Li(3)	90.3(3)
O(3)–Li(2)	1.948(10)	Li(1)–N(2)–Li(3)	94.4(4)
N(1)–Li(2)	2.065(10)	Te(1)–N(3)–Li(3)	90.6(3)
N(1)–Li(1)	2.079(10)	Te(1)–N(3)–Li(2)	90.9(3)
N(2)–Li(1)	2.058(10)	Li(3)–N(3)–Li(2)	95.5(4)
N(2)–Li(3)	2.061(10)	N(2)–Li(1)–N(1)	87.8(4)
N(3)–Li(3)	2.057(10)	N(2)–Li(1)–I(1)	101.3(4)
N(3)–Li(2)	2.067(10)	N(1)–Li(1)–I(1)	100.2(4)
		N(1)–Li(2)–N(3)	86.5(4)
		N(3)–Li(3)–I(1)	99.2(4)
		N(2)–Li(3)–I(1)	101.3(4)

coordinated to one THF molecule. In effect, the LiI template stabilizes a monomeric fragment of the dimer **2**. As indicated by the ^1H NMR data (see Table 1) and CHN analyses (see Experimental Section), there is also one *n*-hexane molecule for two molecules of **4c** in the unit cell. The solid-state structure is close to the ideal C_3 symmetry that is implied by the ^1H , ^{13}C , and ^7Li NMR data (vide supra), but one of the Li–I bonds is significantly shorter [2.901(10) Å] than the other two [2.956(10) and 2.958(10) Å]. These bond lengths are similar to those reported for $d(\text{Li}–\text{I})$ in the sulfur analogue $[(\text{THF})_3\text{Li}_3(\mu_3\text{-I})\{\text{S}(\text{N}^t\text{Bu})_3\}]$, in which two short and one relatively long Li–I bonds are observed (2.912(8) and 2.960(12) Å, respectively).⁸ The mean Te–N distance of 1.979 Å in **4c** is unchanged as compared to the value of 1.976(2) Å found for the dimeric cluster **2**.^{5b} The Li–N distances for the four-coordinate Li^+ ions in **4c** fall within a narrow range, 2.057(10)–2.079(10) Å, with a mean value of 2.064 Å. As expected, this is somewhat longer than the distances found for the three-coordinate Li^+ ions in **2**, which form two short Li–N linkages (mean values 1.977(10) and 1.988(10) Å) and one relatively long Li–N bond (2.147(10) and 2.073(9) Å).^{5b} The mean bond angle $\angle\text{NTeN}$ of 92.02° in **4c** is significantly constrained as compared to the corresponding value of 100.4° for $\angle\text{NSN}$ in the sulfur analogue of **4c**.⁸ The $\angle\text{NTeN}$ value is close to 90° in **4c**, which implies that the lone pair on Te has almost pure s character and, hence,

(28) Although many examples of the incorporation of in situ generated lithium halides into polycyclic structures have been reported, there are only a few instances in which the entrapment of LiX molecules results a *direct reaction* with the alkali halide.²² See also: Veith, M.; Hobein, P.; Huch, V. *J. Chem. Soc., Chem. Commun.* **1995**, 213.

(29) Fleischer, R.; Stalke, D. *Coord. Chem. Rev.* **1998**, 176, 431.

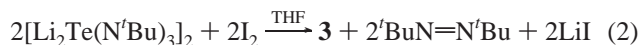
the Lewis base character of the $\text{Te}(\text{N}^t\text{Bu})_3^{2-}$ dianion is weak. Coordination through the Te center is less likely to be observed for **4c** than for the S analogue.^{8,29}

Reactions of $[\text{Li}_2\text{Te}(\text{N}^t\text{Bu})_3]_2$ with (a) Oxygen and (b) Iodine. To compare the behavior of **2** upon oxidation with the behavior of the S and Se analogues of **2**,^{8–10} the reactions of **2** with dry oxygen and iodine were investigated. The oxidation of a toluene solution of **2**, by dry air at 25 °C, was monitored by ESR spectroscopy. The formation of a radical species was evident from the appearance of a septet of decuplets, with ESR parameters $g = 2.00506$, $a(^{14}\text{N}) = 5.26$ G, $a(^7\text{Li}) = 0.69$ G. This spectrum is comparable to those found for the corresponding sulfur- and selenium-containing radicals identified previously as $\{\text{Li}_3[\text{E}(\text{N}^t\text{Bu})_3]_2\}^{\bullet}$ (E = S, Se).^{8,9} Over a period of ca. 1 h, the seven-line spectrum is replaced by a spectrum that is primarily a triplet (1:1:1) of quartets ($g = 2.00620$, $a(^{14}\text{N}) = 13.35$ G, $a(^7\text{Li}) = 1.03$ G). This pattern implies the formation of a radical in which the unpaired electron interacts with one nitrogen (^{14}N , 99.6%, $I = 1$) and two lithium atoms (^7Li , 92.6%, $I = 3/2$). A weaker, poorly resolved five-line spectrum ($g = 2.006$, $a(^{14}\text{N}) = 13.6$ G), tentatively assigned to the radical anion $[\text{OTe}(\text{N}^t\text{Bu})_2]^{\bullet-}$, was superimposed on the three-line spectrum. The evolution of a five-line spectrum ($g = 2.009$, $a(^{14}\text{N}) = 13.4$ G), followed by a three-line spectrum ($g = 2.0095$, $a(^{14}\text{N}) = 15.4$ G), was also observed for the corresponding selenium system but, in that case, the hyperfine splitting by ^7Li was not resolved.⁹ The formation of the radical showing the three-line ESR spectrum occurs more rapidly in *n*-hexane.

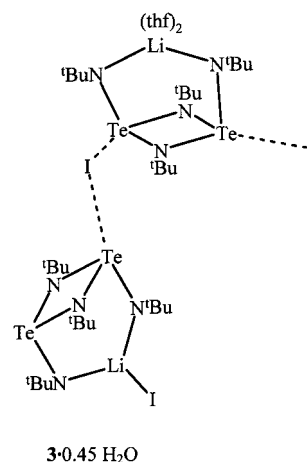
A preparative scale oxidation of **2** was attempted using a solution of I_2 in THF as the oxidant. The major product of this reaction was identified as **3**. Recrystallization of this product, from THF over a period of ca. 3 weeks in an inert atmosphere glovebox, produced X-ray quality crystals containing 0.45 molecule of H_2O per formula unit.³⁰ The cell constants for **3** and **3**·0.45 H_2O are similar and the space groups are identical. The metrical parameters for the tellurium diimide ligands are also alike. As a consequence of a weak interaction between the water molecules and the lithium atom of the coordinated LiI molecule [$d(\text{Li}\cdots\text{O}) = 2.590$ Å], the Li–I distance in **3**·0.45 H_2O is elongated to 2.917(17) Å [cf. 2.695(8) Å in **3**]. An additional difference between the two structures involves the weak $\text{Te}\cdots\text{I}$ contacts. The I^- counterions in **3**·0.45 H_2O behave as μ_2 rather than μ_3 bridges, which is the result of the different relative orientations of the $[\text{Li}(\text{THF})_2]^+$ cation and the adduct $\mathbf{1}\cdot\text{LiI}$. Two independent clusters are centered around the midpoint of the *c* axis, thus forming a twelve-membered $\text{Te}_6\text{Li}_2\text{I}_4$ ring. In

contrast to **3**, however, these two clusters are not linked via $\text{Te}\cdots\text{I}$ contacts. Full details of the structure of **3**·0.45 H_2O have been deposited as Supporting Information.

In summary, the oxidation of **2** by I_2 produces the tellurium diimide dimer **1** and, presumably, $^t\text{BuN}=\text{N}^t\text{Bu}$ (eq 2) rather than



the tellurium(VI) triimide $\text{Te}(\text{N}^t\text{Bu})_3$. In the presence of LiI formed during the reaction, the chelating ligand **1** forms the complex **3**.



Conclusions

The first example of the chelating behavior of the dimeric tellurium diimide ligand **1** toward a single metal center is found in complex **3**, which is prepared by the direct reaction of **1** with LiI in THF, or by the attempted oxidation of $[\text{Li}_2\text{Te}(\text{N}^t\text{Bu})_3]_2$ (**2**) with I_2 . In addition to coordination to LiI and $\text{Li}(\text{THF})_2^+$ fragments, the chelating ligands in **3** are linked by two types of $\text{Te}\cdots\text{I}$ interactions to give an extended structure. The direct reaction of lithium halides with **2** in THF disrupts the dimeric structure to give adducts with a distorted cubic structure that incorporates one molecule of lithium halide.

Acknowledgment. We thank the NSERC Canada for financial support and Dr. R. MacDonald (University of Alberta, Canada) for X-ray data collection of **3**. Helpful discussions of the ESR spectra with Dr. R. T. Boeré (University of Lethbridge, Canada) are gratefully acknowledged.

Supporting Information Available: X-ray crystallographic files, in CIF format. This material is available free of charge via the Internet at <http://pubs.acs.org>.

IC000785+

(30) The source of the water molecules was presumably incompletely dry solvent. Crystal data for **3**·0.45 H_2O : triclinic, space group *P1*, $a = 10.1502(6)$ Å, $b = 15.7212(8)$ Å, $c = 18.9175(11)$ Å, $\alpha = 86.371(1)^\circ$, $\beta = 84.321(1)^\circ$, $\gamma = 82.930(1)^\circ$, $V = 2977.1(3)$ Å³, $Z = 2$, $T = -80$ °C.